

Einstein-Gauss-Bonnet Cosmology Confronted with Observations

Sergei D. Odintsov,^{1,2,*} V.K. Oikonomou,^{3,†} and German S. Sharov^{4,5,‡}

¹*Institut de Ciències de l'Espai, ICE/CSIC-IEEC, Campus UAB,
Carrer de Can Magrans s/n, 08193 Bellaterra (Barcelona), Spain*

²*Institució Catalana de Recerca i Estudis Avançats (ICREA),
Passeig Luis Companys, 23, 08010 Barcelona, Spain*

³*Physics Department, Observatory, Aristotle University of Thessaloniki*

⁴*Tver state university, Sadovyy per. 35, 170002 Tver, Russia*

⁵*International Laboratory for Theoretical Cosmology,
Tomsk State University of Control Systems and Radioelectronics (TUSUR), 634050 Tomsk, Russia*

Several models within the framework of Einstein-Gauss-Bonnet gravities are considered with regard their late-time phenomenological viability. The models contain a non-minimally coupled scalar field and satisfy a constraint on the scalar field Gauss-Bonnet coupling, that guarantees that the speed of the tensor perturbations is equal to the speed of light. The late-time cosmological evolution of these Einstein-Gauss-Bonnet models is confronted with the observational data including the Pantheon plus Type Ia supernovae catalogue, the Hubble parameter measurements (cosmic chronometers), data from cosmic microwave background radiation (CMB) and baryon acoustic oscillations (BAO) including the latest measurements from Dark Energy Spectroscopic Instrument (DESI). Among the considered class of models some of them do not fit the CMB and BAO data. However, there exists some models that generate a viable Einstein-Gauss-Bonnet scenario with well-behaved late-time cosmological evolution that fits the observational data essentially better in comparison to the standard Λ -Cold-Dark-Matter model.

PACS numbers:

I. INTRODUCTION

Theoretical cosmology has an elevated role in modern theoretical physics. The observational data in the last two decades have been cataclysmic offering modern cosmologists the possibility to find suitable models for the description of, mainly, the late Universe, and of course the early Universe. The observations originate from the cosmic microwave background (CMB) radiation data [1], but also from other sources, like the latest Pantheon plus data [2] from Type Ia supernovae (SNe Ia) and also from measurements from Dark Energy Spectroscopic Instrument (DESI) [3] and finally data from baryon acoustic oscillations (BAO). These data strongly challenge the benchmark model for the description of the post-recombination Universe, the Λ -Cold-Dark-Matter model (Λ CDM). On the other hand, the Λ CDM model fits extremely well with the CMB, but there seem to be strong tensions between the local and global measurements of the Hubble constant, challenging the Λ CDM. Indeed, there is a discrepancy of more than 4σ between Λ CDM-based Planck estimations [1] of the Hubble constant and its measurements by SH0ES group [5]. Thus the Λ CDM is challenged to say the least.

However, due to the incredible fitting of the Λ CDM with the CMB, it seems that it is not a model to resent, but should be a model to start with, keeping the good features of it, and refining or eliminating the undesirable features of it. More importantly, the shortcomings of the Λ CDM strongly indicate one thing, that General Relativity (GR) is not able to perfectly describe the post-recombination Universe. The Λ CDM model is based on the foundations of GR, so the tensions mean that GR needs to be modified. There are also other issues that add up to this line of reasoning, for example the fact that the Planck 2018 data [1] allow the dark energy equation of state to cross the phantom divide line, which simply indicates that in terms of a GR theory one needs phantom scalar fields to consistently produce a phantom equation of state. Also the DESI 2024 data [3] indicate a dynamical dark energy era, contrary to the Λ CDM evolution, a result that is confirmed up to 4.2σ statistical confidence in the remarkable findings of the 2025 DESI release [4]. Thus apparently GR is challenged and it is probable hereafter, not possible, that extensions are needed to supplement it, for the moment at large scales physics. There are however many theoretical frameworks that emulate the Λ CDM model regarding the late-time evolution, while being parallelized with the observational data that

*Electronic address: odintsov@ice.csic.es

†Electronic address: v.k.oikonomou1979@gmail.com; voikonomou@gapps.auth.gr

‡Electronic address: sharov.gs@tversu.ru

challenge the Λ CDM model. Modified gravity is the main proponent of this class of Λ CDM-emulator theories, see [6–9] for reviews on the subject. In the recent literature, it has been shown that one of the most mainstream theories of modified gravity, namely $f(R)$ gravity, can fit the observational data much more successfully compared to the Λ CDM model, see for example [10], see also Refs. [11–38] for alternative viewpoints on this line of research. There are several theories of modified gravity which are used and studied in the literature, but only two stand out from a theoretical point of view. These are $f(R)$ gravity theories, which contain Ricci scalar corrections [39–51] and Einstein-Gauss-Bonnet (EGB) theories containing the Gauss-Bonnet (GB) invariant [52–94]. Both have a string theory or a quantum gravity origin. Indeed, it is known that a scalar field in its vacuum configuration can receive quantum corrections at one loop which contain Gauss-Bonnet terms [95, 96] and $f(R)$ gravity terms. In addition, both these theories can offer a unique framework for which the unified description of the dark energy and the inflationary era is realizable. The $f(R)$ gravity confrontation with the observational data was presented in our previous work [10], and in this work the focus shall be on EGB theories. The GB term is a topological invariant in four dimensions, so any linear term in the action turns out a total derivative and thus the GB term does not affect the field equations. But researchers suggested several ways to include the GB term into a gravitational theory: (a) models with Lagrangians nonlinear with respect to the Ricci scalar (modified GB gravities) [52–59]; (b) models with additional spatial dimensions [60–62] and (c) theories including scalar fields coupled to the GB term [63–94]. In this paper, we concentrate on this very last class of GB theories with the GB term being coupled to a scalar field. These models are actually called EGB theories or scalar GB theories [65–94]. These scenarios can potentially describe correctly both the early and late-time era. Usually EGB theories are studied with regard to their inflationary phenomenology [58, 59, 69–81, 85–89]. However, back in 2017 the GW170817 event casted doubt on the theoretical consistency of EGB theories, since these predict a speed of tensor perturbations distinct from that of light. A refinement was proposed in the literature by some of us, and specifically in the articles [76–82, 89] we considered EGB gravities under an important constraint on the coupling factor $\xi(\phi)$ connecting the scalar field ϕ and the GB term: this constraint results from the condition of equality the speed of gravitational waves and the speed of light. This condition appears from the analysis of events with detected gravitational waves (GW), in particular, the GW170817 neutron star merger event by the LIGO/VIRGO collaboration [97] indicated that the GW speed should nearly coincide with that of the light [76, 77]. In this article, we consider a class of EGB model which belong to the class of theories that align with the GW170817 event, studied and developed in Refs. [76–82, 89]. We analyze some EGB models proposed in Refs. [80–82, 89, 92, 93] and then concentrate on the most successful scenario and by using observational datasets that include Pantheon+ SNe Ia catalogue, CMB data, measurements of the Hubble parameter $H(z)$ (Cosmic Chronometers) and DESI BAO data. The viable EGB model appears to be essentially more successful than the standard Λ CDM model in fitting this observational data.

The paper is organized as follows: the basic features and equations of EGB gravity and the class of viable models are considered in section II. In Sect. III, the observational data for SNe Ia, BAO, CMB and $H(z)$ is shown up as well as the corresponding χ^2 functions for fitting the model. In Sect. IV we select the most successful EGB scenario and in the next section describe its predictions and compare them with the results of Λ CDM model. The conclusions and final discussion are made in Sect. VI.

II. ESSENTIAL FEATURES OF EINSTEIN-GAUSS-BONNET GRAVITY

In this section we shall present the theoretical framework of GW170817-compatible EGB gravity, the action of which is [89–93],

$$S = \int d^4x \sqrt{-g} \left(\frac{R}{2\kappa^2} f(\phi) - \frac{1}{2} \partial_\mu \phi \partial^\mu \phi - V(\phi) - \xi(\phi) \mathcal{G} + \mathcal{L}_{(m)} \right), \quad (1)$$

where $\kappa^2 = 8\pi G$, ϕ is a scalar field, $R = R^\mu_\mu$ is the Ricci scalar, $\mathcal{L}_{(m)}$ is the matter Lagrangian and \mathcal{G} is the Gauss-Bonnet topological invariant expressed via the Ricci tensor $R_{\mu\nu}$ and the Riemann curvature tensor $R_{\mu\nu\sigma\rho}$. In many papers [69–88] a more simple form of EBG gravity with the factor $f(\phi) = 1$ is explored,

$$S = \int d^4x \sqrt{-g} \left(\frac{R}{2\kappa^2} - \frac{1}{2} \partial_\mu \phi \partial^\mu \phi - V(\phi) - \xi(\phi) \mathcal{G} + \mathcal{L}_{(m)} \right), \quad (2)$$

In this paper, we will work with both actions (1) and (2) in the framework of a flat Friedman-Lemaître-Robertson-Walker (FLRW) metric

$$ds^2 = -dt^2 + a(t)^2 \delta_{ij} dx^i dx^j, \quad (3)$$

where $a(t)$ is the scale factor, and for the FLRW spacetime, the Ricci scalar and the Gauss-Bonnet invariant take the following form,

$$R = 6(2H^2 + \dot{H}), \quad \mathcal{G} = 24H^2(H^2 + \dot{H}), \quad H = \frac{\dot{a}}{a}.$$

Varying the action (1) with respect to the metric and to ϕ we obtain the field equations [89–93]:

$$3fH^2 = \kappa^2 \left(\rho + \frac{1}{2}\dot{\phi}^2 + V + 24\dot{\xi}H^3 \right) - 3H\dot{f}, \quad (4)$$

$$-2f\dot{H} = \kappa^2 \left[\rho + P + \dot{\phi}^2 - 16\dot{\xi}H\dot{H} - 8H^2(\ddot{\xi} - H\dot{\xi}) \right] + \ddot{f} - H\dot{f}, \quad (5)$$

$$\ddot{\phi} + 3H\dot{\phi} + V'(\phi) - \frac{f'(\phi)}{2\kappa^2}R + \xi'(\phi)\mathcal{G} = 0. \quad (6)$$

Here ρ and P are the matter density and pressure respectively of the matter fluids, matter is the essential component during the late-time epoch that is under consideration in this research. Note that Eq. (6) is obtained by combining the first two equations (4) and (5) and may be omitted, but we will use it in our considerations.

In this paper, we impose the mentioned constraint on the coupling function $\xi(\phi)$ coming from the equality of the GW speed and speed of light, in order for the EGB theory to be GW170817-compatible. This constraint is equivalent to the following differential equation [76–82, 89]:

$$\ddot{\xi} = H\dot{\xi}, \quad (7)$$

which can be easily integrated to be expressed in terms of the scale factor

$$\dot{\xi} = C \cdot a, \quad C = \text{const}. \quad (8)$$

For any concrete EGB scenario we should choose the factor $f(\phi)$, the potential $V(\phi)$ and describe the matter content ρ and P . Then we can integrate the system of equations (4)–(6) under the restrictions (7), (8) with given initial conditions at the present time t_0 . In particular, some EGB scenarios under the restriction (7) were tested with the statefinder parameter analysis in comparison to Λ CDM model for late-time cosmology [92]. In Ref. [93] we explored some EGB scenarios with Eq. (7) solving the system (4)–(6) in confrontation with late-time observations. In that paper the matter components were assumed as $\rho = \rho_m + \rho_r$, where ρ_m describes baryons and cold dark matter ($\rho_m \simeq \rho_b + \rho_c$) and ρ_r refers to relativistic particles (photons and neutrinos). For each matter component its continuity equation,

$$\dot{\rho}_i + 3H(\rho_i + P_i) = 0$$

can be solved and we obtain,

$$\rho = \rho_m^0 (a^{-3} + X_r a^{-4}), \quad (9)$$

where $X_r = \rho_r^0/\rho_m^0$, the index 0 denotes present day values (at $t = t_0$) and $a(t_0) = 1$. To minimize the number of free model parameters, we fix the radiation to matter ratio as estimated by Planck [98, 99]:

$$X_r = \frac{\rho_r^0}{\rho_m^0} = 2.9656 \times 10^{-4}. \quad (10)$$

Models from the considered class can be viable if (a) they allow physical solutions and (b) these solutions satisfy observational limitations. In the next section we describe actual observational data used in this paper.

III. OBSERVATIONAL DATA

We test the EGB models (1), (2) with observational data including the Pantheon+ sample database [2] of Type Ia Supernovae (SNe Ia), the Hubble parameter $H(z)$ measurements, observable parameters of Cosmic Microwave Background radiation (CMB) and Baryon Acoustic Oscillations (BAO) with the latest BAO measurements from Dark Energy Spectroscopic Instrument (DESI) collaboration [3]. To confront any model with these observations we

use some methods developed previously in papers [99–101]).

For SNe Ia we use $N_{\text{SN}} = 1701$ Pantheon+ datapoints [2] with information of the distance moduli μ_i^{obs} at redshifts z_i from 1550 SNe Ia and compute the χ^2 function:

$$\chi_{\text{SN}}^2(\theta_1, \dots) = \min_{H_0} \sum_{i,j=1}^{N_{\text{SN}}} \Delta\mu_i (C_{\text{SN}}^{-1})_{ij} \Delta\mu_j, \quad (11)$$

$$\Delta\mu_i = \mu^{\text{th}}(z_i, \theta_1, \dots) - \mu_i^{\text{obs}}.$$

Here θ_j are free model parameters, the Hubble constant H_0 is considered as a nuisance parameter, C_{SN} is the $N_{\text{SN}} \times N_{\text{SN}}$ covariance matrix and μ^{th} are the theoretical values for the distance moduli depending on redshift $z = a^{-1} - 1$:

$$\mu^{\text{th}}(z) = 5 \log_{10} \frac{(1+z) D_M(z)}{10 \text{pc}}, \quad D_M(z) = c \int_0^z \frac{d\tilde{z}}{H(\tilde{z})}. \quad (12)$$

In this paper, we use the Hubble parameter $H(z)$ measurements named ‘‘Cosmic Chronometers’’ (CC): they are made by the method of different ages Δt for galaxies with known variations of redshifts Δz . The values $H(z)$ are estimated via the relation:

$$H(z) = \frac{\dot{a}}{a} \simeq -\frac{1}{1+z} \frac{\Delta z}{\Delta t}.$$

For the present analysis $N_H = 32$ data points of $H^{\text{obs}}(z_i)$ are used with references in the previous papers [101]). The χ^2 function for $H(z)$ fittings yields:

$$\chi_H^2 = \sum_{i=1}^{N_H} \left[\frac{H^{\text{obs}}(z_i) - H^{\text{th}}(z_i; \theta_k)}{\sigma_{H,i}} \right]^2. \quad (13)$$

CMB observational parameters are related to the photon-decoupling epoch at redshifts close to $z_* = 1089.80 \pm 0.21$ and are given by the vector [1]:

$$\mathbf{x} = (R, \ell_A, \omega_b), \quad R = \sqrt{\Omega_m^0} \frac{H_0 D_M(z_*)}{c}, \quad \ell_A = \frac{\pi D_M(z_*)}{r_s(z_*)}, \quad \omega_b = \Omega_b^0 h^2 \quad (14)$$

whose estimations are [102]:

$$\mathbf{x}^{\text{Pl}} = (R^{\text{Pl}}, \ell_A^{\text{Pl}}, \omega_b^{\text{Pl}}) = (1.7428 \pm 0.0053, 301.406 \pm 0.090, 0.02259 \pm 0.00017). \quad (15)$$

The comoving sound horizon $r_s(z_*)$ is obtained by the integral [101]):

$$r_s(z) = \int_z^\infty \frac{c_s(\tilde{z})}{H(\tilde{z})} d\tilde{z} = \frac{1}{\sqrt{3}} \int_0^{1/(1+z)} \frac{da}{a^2 H(a) \sqrt{1 + [3\Omega_b^0 / (4\Omega_\gamma^0)] a}}, \quad (16)$$

with the estimation of z_* given in Refs. [102]. The reduced baryon fraction ω_b is considered as the nuisance parameter in the following χ^2 function:

$$\chi_{\text{CMB}}^2 = \min_{\omega_b, H_0} \Delta \mathbf{x} \cdot C_{\text{CMB}}^{-1} (\Delta \mathbf{x})^T, \quad \Delta \mathbf{x} = \mathbf{x} - \mathbf{x}^{\text{Pl}}, \quad (17)$$

where $C_{\text{CMB}} = \|\tilde{C}_{ij} \sigma_i \sigma_j\|$ is the covariance [99, 102]. For the Baryon Acoustic Oscillations (BAO) we consider new data from Dark Energy Spectroscopic Instrument (DESI) Data Release 1 [3] is considered. We calculate and compare with measurements the value

$$d_z(z) = \frac{r_s(z_d)}{D_V(z)}, \quad D_V(z) = \left[\frac{cz D_M^2(z)}{H(z)} \right]^{1/3}, \quad (18)$$

where z_d being the redshift at the end of the baryon drag era whereas the comoving sound horizon $r_s(z)$ is obtained as the integral (16). The estimations for z_d and for the ratio of baryons and photons $\Omega_b^0 / \Omega_\gamma$ are fixed by the Planck 2018 data [1].

In this paper, we use 6 BAO datapoints, shown in Table I and provided by DESI DR1 data [3]. These measurements include BAO data from clustering of galaxies, quasars and the Lyman- α forest in the redshift range $0.1 < z < 4.16$. The χ^2 function is

$$\chi_{\text{BAO}}^2(\theta_1, \dots) = \sum_{i=1}^6 \left[\frac{d_z^{\text{obs}}(z_i) - d_z^{\text{th}}(z_i, \dots)}{\sigma_{d_z, i}} \right]^2. \quad (19)$$

| | | | | | | |
|------------------|---------------------|---------------------|---------------------|----------------------|----------------------|-----------------------|
| z_{eff} | 0.295 | 0.51 | 0.706 | 0.93 | 1.317 | 2.33 |
| z range | 0.1 - 0.4 | 0.4 - 0.6 | 0.5 - 0.8 | 0.8 - 1.1 | 1.1 - 1.6 | 1.77 - 4.16 |
| d_z | 0.1261 ± 0.0024 | 0.0796 ± 0.0018 | 0.0629 ± 0.0014 | 0.05034 ± 0.0008 | 0.04144 ± 0.0011 | 0.03173 ± 0.00073 |

TABLE I: DESI DR1 BAO data.

Then, the free parameters for a given EGB model should be fitted with all these sources of data. In the next section, we estimate viability of some EGB scenarios in this test.

IV. VIABLE EGB MODELS

We begin our analysis from the most popular EGB models with the action (2) [74–84]. Their dynamics will be determined if we impose the condition (7) or $\dot{\xi} = Ca$ and fix the potential $V(\phi)$. In the mentioned papers the authors explore different variants of $V(\phi)$ having a preference for power-law and exponential potentials that may be written in the following common form:

$$V(\phi) = V_0 \left(\frac{\phi}{\phi_0} \right)^\alpha, \quad (20)$$

$$V(\phi) = V_0 \exp[\tilde{\alpha}(\phi - \phi_0)]. \quad (21)$$

Recall that the index “0” denotes the present day values of variables. Instead of the Hubble parameter $H(t)$, the scalar $\phi(t)$, its derivative $\dot{\phi}$, the constants ρ_m^0 , V_0 , C it is convenient to use dimensionless variables and parameters:

$$E = \frac{H}{H_0}, \quad \varphi = \kappa\phi, \quad \psi = \frac{\kappa}{H_0}\dot{\phi}; \quad \Omega_m^0 = \frac{\kappa^2 \rho_m^0}{3H_0^2}, \quad \Omega_V = \frac{\kappa^2 V_0}{3H_0^2}, \quad \lambda = \kappa^2 H_0 C. \quad (22)$$

In this notation the potentials (20) and (21) take the common form

$$V(\varphi) = V_0 \cdot v(\varphi), \quad v(\varphi) = (\varphi/\varphi_0)^\alpha \quad \text{or} \quad v(\varphi) = \exp[\alpha(\varphi - \varphi_0)]$$

the condition (8) transforms into $\dot{\xi} = \frac{\lambda}{\kappa^2 H_0} a$, and the system of equations (4)–(6) for the considered case (2) ($f = 1$) can be expressed as:

$$E^2(1 - 8\lambda a E) = \Omega_m^0(a^{-3} + X_r a^{-4}) + \frac{1}{6}\psi^2 + \Omega_V v(\varphi), \quad (23)$$

$$2E \frac{dE}{dx}(1 - 8\lambda a E) = -\Omega_m^0(3a^{-3} + 4X_r a^{-4}) - \psi^2, \quad (24)$$

$$\frac{d\psi}{dx} + 3\psi + 3 \frac{\Omega_V v'(\varphi)}{E} + 24 \frac{\lambda a}{\psi} E^2 \left(E + \frac{dE}{dx} \right) = 0. \quad (25)$$

Here $x = \log a$, $\frac{d}{dt} = H \frac{d}{dx}$, $\psi = E \frac{d\varphi}{dx}$. This system can be solved numerically in the “past” direction starting at the present time as described in Ref. [93]. We fix initial conditions at the present time $t = t_0$ (equivalent to $x = 0$ or $a = 1$), where the following free model parameters should be fixed:

$$E|_{x=0} = 1, \quad \varphi|_{x=0} = \varphi_0, \quad \psi|_{x=0} = \psi_0 = \pm \sqrt{6[1 - 8\lambda - \Omega_m^0(1 + X_r) - \Omega_V]}. \quad (26)$$

For any set of free model parameters Ω_m^0 , Ω_V , H_0 , λ , φ_0 , α for both power-law (20) and exponential (21) potentials we can obtain the solution $E(x)$, $\varphi(x)$ of the system (23)–(25) and (if this solution is physical) compare it with observational data. For this purpose we use the Hubble parameter $E(z)$ or $H(z) = H_0 E(z)$, where $z = a^{-1} - 1 = e^{-x} - 1$.

Our calculations showed that physical solutions describing Pantheon+ SNe Ia data [2] and CC $H(z)$ data exist for both power-law and exponential models (20), (21). If we consider only χ^2 functions for SNe Ia (11) and CC (13) or their sum $\chi_{\text{SN}}^2 + \chi_H^2$, these EGB models appear to be more successful than the standard Λ CDM model with,

$$\frac{H(z)}{H_0} = [\Omega_m^0(a^{-3} + X_r a^{-4}) + \Omega_\Lambda]^{1/2}, \quad \Omega_\Lambda = 1 - \Omega_m^0(1 + X_r). \quad (27)$$

The mentioned Pantheon+ SNe Ia and $H(z)$ observations are related with the late-time epoch at the range $0 < z < 2.5$. However, at more early times (at $z > 100$) for both EGB scenarios (20) and (21) the normalized Hubble parameter $E(x)$ deviates from the Λ CDM expression (27). Such a behavior can be seen in the top-left panel of Fig. 1 for both EGB potentials (20) and (21). On the one hand the Λ CDM normalized Hubble parameter (27) behaves as $E \sim a^{-2}$ before the recombination epoch and $E \simeq \sqrt{\Omega_m^0} \cdot a^{-3/2}$ after (at $10^3 > z \gg 1$ or $-7 > x > -3$); on the other hand both EGB scenarios at high redshifts grow quickly in the power-law manner: $E \sim a^{-3}$. Such a behavior is the consequence of growing value $\psi \sim a^{-3}$ at high redshifts in accordance with Eq. (25) that can be seen in the bottom-right panel of Fig. 1. As the result the term $\frac{1}{6}\psi^2$ becomes dominating in the right hand side of equation (23) that leads to the mentioned growth $E \sim a^{-3}$. The examples in the top-right panel of Fig. 1 show that both EGB scenarios (20) and

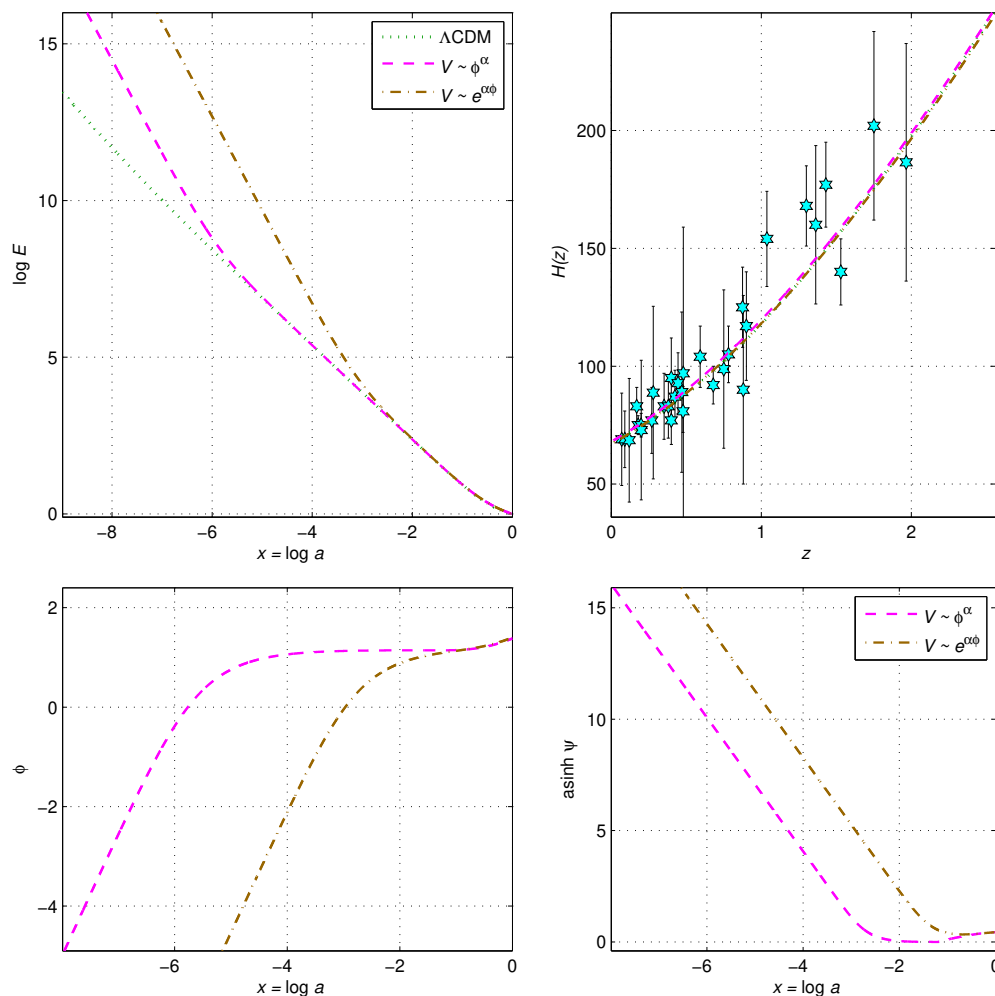


FIG. 1: Evolution of the normalized Hubble parameter $E = H/H_0$ (top-left panel), the Hubble parameter $H(z)$ at small redshifts (top-right panel), the scalar field $\varphi = \kappa\phi$ and its derivative $\psi = E \frac{d}{dx} \varphi$ (bottom panels) versus $x = \log a$ for the EGB models with the power-law and exponential potentials (20), (21) in comparison with the Λ CDM model (27).

(21) can describe CC $H(z)$ data (32 CC datapoints are depicted). This also concerns to Pantheon+ SNe Ia data at the same redshift range $0 < z < 2.5$ and we can achieve better fits for the sum $\chi_{\text{SN}}^2 + \chi_H^2$ compared to the Λ CDM model. In particular, in Fig. 1 the model parameters are chosen near the best fits: $\Omega_m^0 = 0.286$, $H_0 = 68.0 \text{ km (s Mpc)}^{-1}$ for

all models; $\Omega_V = 0.68$, $\varphi_0 = 1.4$ for both EGB scenarios; $\alpha = -1$, $\lambda = -5 \cdot 10^{-6}$ for the power-law and $\alpha = -0.75$, $\lambda = -3 \cdot 10^{-6}$ for the exponential model.

The above described asymptotic behavior $E \sim a^{-3}$ for both EGB scenarios (20) and (21) takes place for any set of free parameters and initial conditions. This said behavior leads to an essential difference in the calculated integral (16) for the comoving sound horizon $r_s(z)$ between these EGB scenarios and the Λ CDM model. The value $r_s(z)$ determines not only theoretical CMB parameter ℓ_A (14) related to the recombination epoch, but also the BAO parameter d_z (18). As the result for EGB scenarios (20) and (21) we have very large discrepancies between theoretical and observational CMB and BAO parameters leading to high values of χ_{BAO}^2 and χ_{CMB}^2 : minima of these χ^2 functions and their sum for the mentioned EGB models exceed the corresponding Λ CDM minima in many orders of magnitude.

Due to this reason the EGB scenarios with the action (2), the condition (8) and potentials (20), (21) (and other physically acceptable potentials) concede to Λ CDM model when we test them with the whole set of SNe Ia, $H(z)$, CMB and BAO observational data. However, among a more wide class of EGB models with the action (1) we can find scenarios with suitable behavior of the Hubble parameter $H(z)$ at high redshifts. In particular, we can consider the model of the type (1) with the factor $f(\phi) = \phi_0/\phi = \varphi_0/\varphi$ explored in the papers [92, 93]. For this model with the corresponding power-law potential $V(\phi) \sim \phi^{-1}$ we use the following terms in the Lagrangian (1):

$$\frac{R}{2\kappa^2}f(\phi) - V(\phi) = \frac{R}{2\kappa^2}\frac{\varphi_0}{\varphi} - V_0\frac{\varphi_0}{\varphi}. \quad (28)$$

For the model (28) under the condition (7) or (8) (restricting the GW speed) in notation (22) the equations (4)–(6) are transformed into the following system:

$$E^2[f(\phi) - 8\lambda aE] = \Omega_m^0(a^{-3} + X_r a^{-4}) + \frac{1}{6}\psi^2 + (\Omega_V + E\psi/\varphi)f(\phi), \quad (29)$$

$$2E\frac{dE}{dx}\left(\frac{\varphi_0}{\varphi} - 8\lambda aE\right) = -\Omega_m^0(3a^{-3} + 4X_r a^{-4}) - \psi^2 + \frac{\varphi_0}{\varphi^2}\left(E\frac{d\psi}{dx} - E\psi - 2\frac{\psi^2}{\varphi}\right), \quad (30)$$

$$\frac{d\psi}{dx} + 3\psi - 3\frac{\Omega_V\varphi_0}{E\varphi^2} + 24\frac{\lambda a}{\psi}E^2\left(E + \frac{dE}{dx}\right) + 3\frac{\varphi_0}{\varphi^2}\left(2E + \frac{dE}{dx}\right) = 0. \quad (31)$$

This system is solved numerically similarly to Eqs. (23)–(25) with the initial conditions similar to (26): $E|_{x=0} = H_0/H_0 = 1$, $\varphi|_{x=0} = \varphi_0$, but with ψ_0 determined by Eq. (29) at $x = 0$:

$$\psi|_{x=0} = -3\varphi_0^{-1} + \sqrt{9\varphi_0^{-2} - 6[\Omega_m^0(1 + X_r) + \Omega_V - 1 + 8\lambda]}. \quad (32)$$

For deriving the solution at every step we calculate $\psi(x)$ and the preliminary value $\varphi(x) = \int \psi E^{-1} dx$, then determine E by solving the equation (29) and redefine $\varphi(x)$. Further, we extract the derivative $\frac{d\psi}{dx}$ from equations (30) and (31) in order to calculate $\psi(x - \Delta x)$ at the next step.

In these calculations we obtained solutions for the EGB model (28) behaving closely to Λ CDM solutions (27) at late and early times. Our results may be confronted with the observational data, and we present this analysis in the following section.

V. FURTHER CONFRONTATION OF VIABLE EGB WITH THE OBSERVATIONAL DATA

To compare the EGB model (28) with the observational datasets described in Sect. III we fit its free parameters

$$\Omega_m^0, \quad \Omega_V, \quad H_0, \quad \lambda, \quad \varphi_0, \quad (33)$$

calculating the corresponding χ_i^2 functions (11), (13), (17), (19) for SNe Ia, $H(z)$, CMB and BAO datasets and the total (summarized) χ_{tot}^2 function:

$$\chi^2 \equiv \chi_{\text{tot}}^2 = \chi_{\text{SN}}^2 + \chi_H^2 + \chi_{\text{BAO}}^2 + \chi_{\text{CMB}}^2. \quad (34)$$

We calculated this χ^2 function for each pair of the free parameters (33) and presented the results in Fig. 2 and Fig. 3 with the contour plots at 1σ (68.27%) and 2σ (95.45%) confidence levels (CL) for two-parameter distributions $\chi^2(\theta_j, \theta_k)$.

In Fig. 2 we compare the EGB model (28) under the condition (8) with the Λ CDM model (27). In the bottom-left panel 1σ and 2σ contours plots are depicted in the plane $\Omega_m^0 - H_0$ of their common parameters for two-parameter distributions. In the EGB case this distribution is the following minimum over other free parameters:

$$\chi^2(\Omega_m^0, H_0) = \min_{\Omega_V, \lambda, \varphi_0} \chi^2(\Omega_m^0, \Omega_V, \lambda, \varphi_0, H_0).$$

The minimum points for $\chi^2(\Omega_m^0, H_0)$ in this panel are labelled with the star for EGB (filled contours) and with the circle for Λ CDM model. In the bottom-right panel of Fig. 2 the one-parameter distributions $\chi^2(H_0)$ (minimized

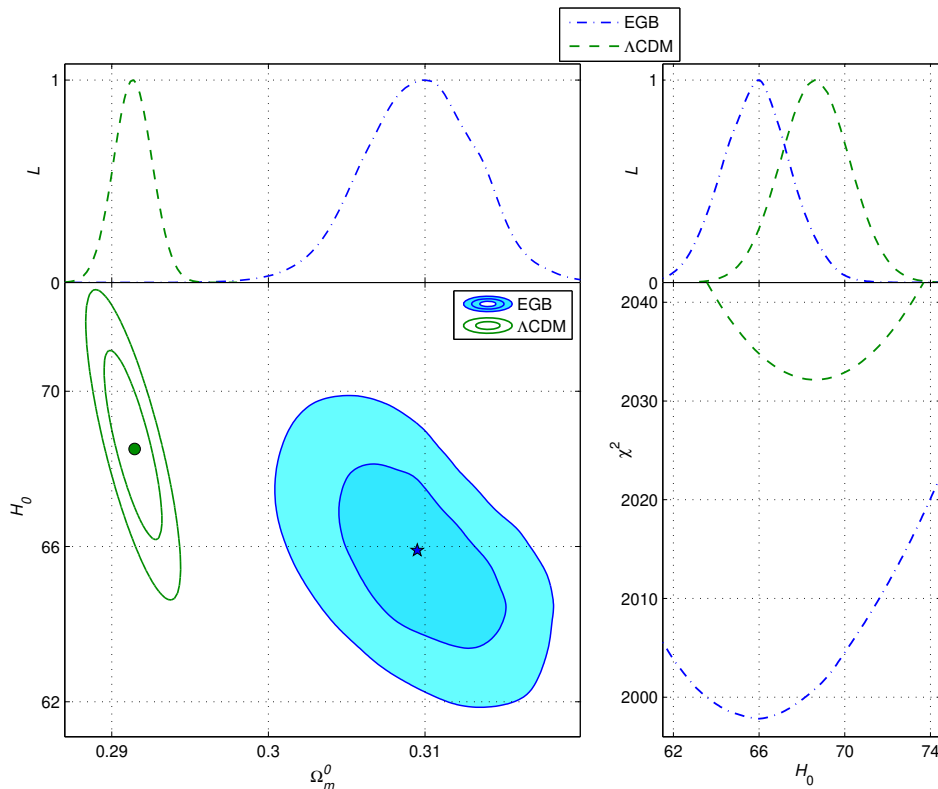


FIG. 2: Contours plots at 1σ and 2σ CL in the $\Omega_m^0 - H_0$ plane, likelihoods $\mathcal{L}(\Omega_m^0)$, $\mathcal{L}(H_0)$ and one-parameter distributions $\chi^2(H_0)$ for the EGB model (28) in comparison with Λ CDM model.

over the rest of the free parameters) for both models are depicted and compared; in the top panels one can see the corresponding likelihoods $\mathcal{L}(\Omega_m^0)$ and $\mathcal{L}(H_0)$, where

$$\mathcal{L}(\theta_k) \propto \exp \left[-\frac{1}{2} \chi^2(\theta_k) \right]. \quad (35)$$

The contours and the predicted best fits for the EGB and Λ CDM models strongly differ in the bottom-left panel of Fig. 2: this difference exceeds 3σ . These best fits deviate especially sharply for the parameter Ω_m^0 : $\Omega_m^0 = 0.2913_{-0.0012}^{+0.0012}$ for Λ CDM and $\Omega_m^0 = 0.3096_{-0.0036}^{+0.0040}$ for EGB. These and other best fits and 1σ errors for the free parameters θ_k are tabulated in Table II, they are obtained from one-parameter distributions $\chi^2(\theta_k)$. From this table and likelihoods $\mathcal{L}(H_0)$ in the top-right panel of Fig. 2 one may conclude that the best fits for the Hubble constant H_0 for both models differ of order 1σ and the EGB model predicts the lowest estimation: $H_0 = 65.90_{-1.54}^{+1.48}$ km/(sMpc).

In the bottom-right panel of Fig. 2 the one-parameter distributions $\chi^2(H_0)$ illustrate the large difference between two considered models: the EGB model (28) appeared to be much more successful in its absolute minimum $\min \chi^2 \simeq 1997.76$ in comparison with the Λ CDM result $\min \chi^2 \simeq 2032.15$. One may conclude that the EGB model fits essentially better the observational data in comparison to Λ CDM model according to the minimum of χ^2 .

Moreover, in order to improve our statistical analysis we can take into account the large number $N_p = 5$ of free parameters (33) for the EGB model, while Λ CDM just contains $N_p = 2$, and consider the Akaike information criterion (AIC parameter) [99]:

$$\text{AIC} = \min \chi^2 + 2N_p \quad (36)$$

and Bayesian information criterion (BIC) [103]

$$\text{BIC} = \min \chi^2 + N_p \cdot \log(N_d), \quad (37)$$

where N_d is the number of data points. In Table II one can see that the advantage of the EGB model (28) in $\min \chi^2$ remains at a high level when we consider both Akaike and Bayesian information criteria. In particular, we see the difference between these models $\Delta\text{AIC} = \text{AIC}_{\text{EGB}} - \text{AIC}_{\Lambda\text{CDM}} = -28.39$ and $\Delta\text{BIC} = \text{BIC}_{\text{EGB}} - \text{BIC}_{\Lambda\text{CDM}} = -12.002$ both in favor of the EGB model (28). The EGB model (28) was analyzed in detail for all pairs of (θ_j, θ_k) its free

| Model | $\min \chi^2/d.o.f$ | AIC | BIC | Ω_m^0 | H_0 | Ω_V | $10^6 \cdot \lambda$ | φ_0 |
|---------------------|---------------------|---------|----------|------------------------------|-------------------------|---------------------------|---------------------------|---------------------------|
| EGB (28) | 1997.76 /1738 | 2007.76 | 2035.074 | $0.3096_{-0.0036}^{+0.0040}$ | $65.90_{-1.54}^{+1.48}$ | $0.789_{-0.014}^{+0.011}$ | $-0.18_{-0.910}^{+0.167}$ | $0.310_{-0.185}^{+0.548}$ |
| ΛCDM | 2032.15 /1741 | 2036.15 | 2047.076 | $0.2913_{-0.0012}^{+0.0012}$ | $68.60_{-1.59}^{+1.62}$ | - | - | - |

TABLE II: Best fits, $\min \chi^2$, AIC and ΔAIC from SNe Ia, $H(z)$, BAO and CMB datasets for the EGB (28) and ΛCDM models.

model parameters (33), these results are reproduced in Fig. 3 in notation of Fig. 2. One can note that the scenario is viable only with small negative values for the parameter λ in the range $-4 \cdot 10^{-6} < \lambda < 0$. This limitation and the condition (8) in the form $\xi = \frac{\lambda}{\kappa^2 H_0} a$ lead to a weakly varying or nearly constant coupling factor ξ with the GB term. The term $8\lambda a E$ in equations (29) and (29) appeared to be small ($|8\lambda a E| \ll 1$) for λ in the mentioned range and other parameters in the limits from Table II at the late epoch $z < 1000$ or $a > 10^{-3}$, because E for viable solutions is close to the ΛCDM expression (27) at this epoch: $E \simeq \sqrt{\Omega_m^0} \cdot a^{-3/2}$. Hence, for $a > 10^{-3}$ the value aE has the upper bound of order $\sqrt{\Omega_m^0} \cdot 10^{3/2}$.

In the top-right panel in Fig. 3 the evolution of the scalar field $\varphi = \varphi(x)$ is depicted in the case of the best fitted model parameters from Table II. We see that the scalar field remains almost constant $\varphi \simeq \varphi_0 = 0.31$ for redshifts $z < 1000$ or $-6.9 < x < 0$ and deviates from its present value φ_0 only at more early times, when $\psi = H_0^{-1} \dot{\varphi}$ essentially deviates from zero. Under these circumstances ($\varphi \simeq \varphi_0$, $\psi \simeq 0$, $|8\lambda a E| \ll 1$) at late times after the recombination epoch the dynamical equation (29) becomes close to the ΛCDM equation (27), where the parameter Ω_V plays the role of Ω_Λ . However, Ω_V (22) in these EGB scenarios is a free model parameter, the sum $\Omega_m^0 + \Omega_V$ is not limited in contrast to ΛCDM model. In particular, for the EGB model (28) the sum $\Omega_m^0 + \Omega_V$ of the best fitted values from Table II exceeds 1, it is true for 2σ CL domain in the $\Omega_m^0 - \Omega_V$ panel in Fig. 3. This freedom in choosing Ω_V , obviously, leads to the mentioned success of the model (28) in comparison with ΛCDM model in minimizing χ^2 . Additional degrees of freedom in the EGB scenario (28) lead to lower minimum of χ^2 and enlarges the best fit of Ω_m^0 (with increased 1σ error $\Delta\Omega_m^0$) in comparison with ΛCDM model. The free model parameters λ and φ_0 are correlated if we search minimal values of χ^2 : if $|\lambda|$ tends to zero, the corresponding fitted values of φ_0 also diminish. The best fits of these parameters $|\lambda| \simeq 1.8 \cdot 10^{-7}$ and $\varphi_0 \simeq 0.31$ are attracted to zero borders of their domains in Fig. 3.

VI. CONCLUSIONS

In this paper, some scenarios of viable GW170817-compatible EGB gravity have been studied and tested with observational data, regarding their late-time phenomenology. These models include in their Lagrangian a linear combination of the Ricci scalar and the Gauss-Bonnet term particularly coupled to a scalar field ϕ . These models have been explored under the condition (7) on the coupling function $\xi(\phi)$ coming from coincidence of the speed of gravitational waves and the speed of light [77–80]. Scenarios of this type have been considered in the literature, some of them can have suitable solutions at late-times but with singularities or instabilities at larger redshifts [92, 93].

In the first part of this paper, we have studied EGB models with the gravitational action (2) where the Ricci scalar in Lagrangian has a minimal coupling to the scalar field. We considered scenarios with different types of the potential $V(\phi)$, in particular, with power-law (20) and exponential potential (21). These EGB scenarios have solutions describing $H(z)$ and Pantheon+ SNe Ia observational data (related to redshifts $0 < z < 2.5$) better than ΛCDM model. However, these solutions for the potentials (20), (21) and other viable potentials at high redshifts have too quick growth of the Hubble parameter: $H(a) \sim a^{-3}$ (see Fig. 1). Because of this asymptotic behavior we can not describe satisfactory CMB and BAO observational data with the EGB models coming from the action (2) under the condition (7).

To avoid this drawback we have studied a more wide class of EGB models determined by action (1) and the constraint (7). The model (28) from this class with the factor $f(\phi) = \phi_0/\phi$ and the similarly behaving potential $V(\phi) = V_0\phi_0/\phi$ appeared to be successful in tests with all the observational data used in the paper: the Pantheon+ SNe Ia data, $H(z)$ measurements, CMB and DESI BAO data. This model, previously considered in papers [92, 93], includes solutions with a regular at all redshift ranges considered. The model (28) fits the mentioned observational data used essentially better than ΛCDM model. The results of the fittings comparison with ΛCDM model are summarized in Table II and depicted in Figs. 2, 3.

To compare the EGB scenario (28) and ΛCDM model we note that the absolute minima of the total χ^2 function

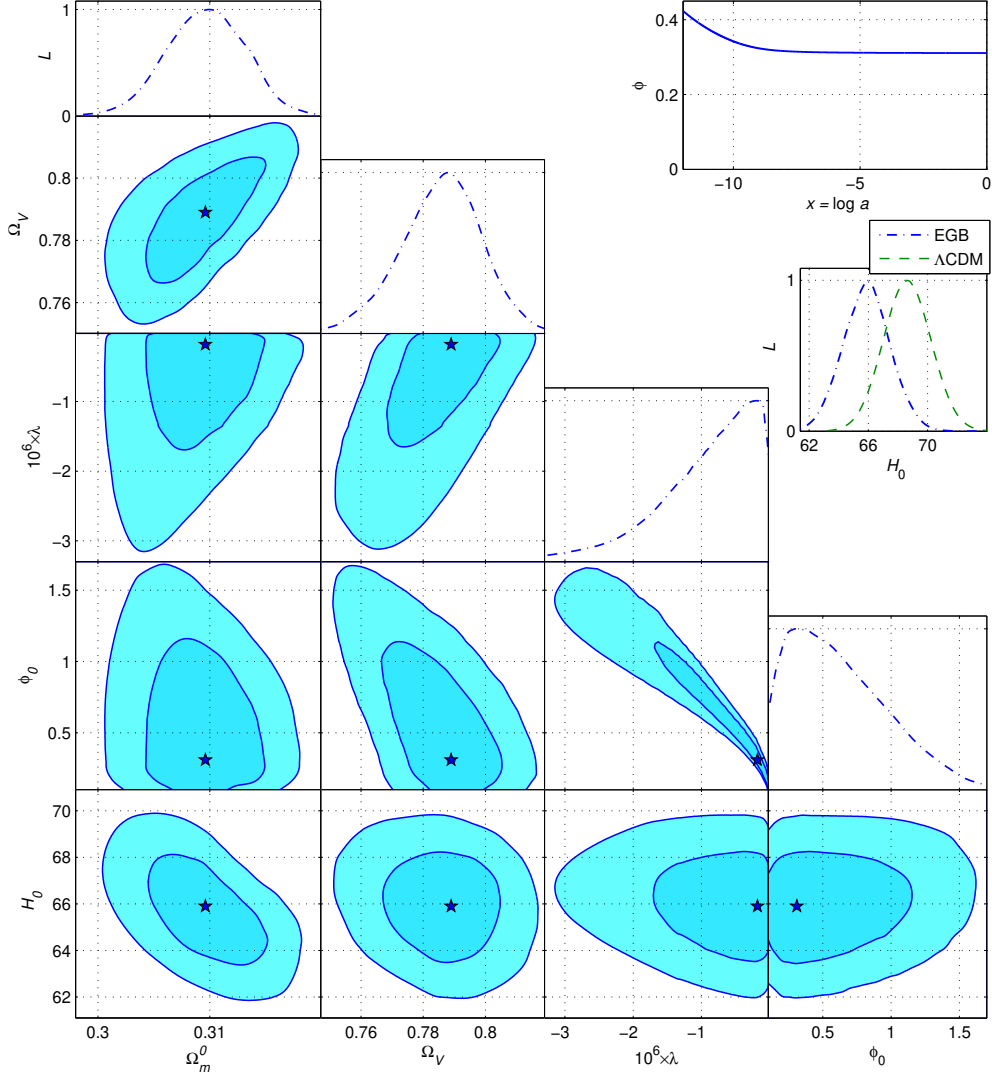


FIG. 3: EGB model (28): 1σ and 2σ contours plots, likelihoods for all free parameters and evolution of the scalar field φ in the top-right panel.

(34) radically differ: the EGB result $\min \chi^2 \simeq 1997.76$ is lower than the Λ CDM value $\min \chi^2 \simeq 2032.15$ with the large difference 34.39, that can be estimated as more than 3σ CL in Fig. 2. This advantage of the EGB scenario (28) remains despite the large number $N_p = 5$ of its free parameters, when we consider Akaike (36) and Bayesian (37) information criteria [103]. The difference between results of these models $\Delta\text{AIC} = \text{AIC}_{\text{EGB}} - \text{AIC}_{\Lambda\text{CDM}} = -28.39$ and $\Delta\text{BIC} = -12.002$ remains large in favor of the EGB model (28). Note that in our previous paper [93] this EGB model did not have this advantage: the AIC value for Λ CDM model was better than for the EGB scenario. These changes are connected with the latest SNe Ia Pantheon+ 1701 datapoints [2], whereas in Ref. [93] we used 1048 datapoints of the previous catalogue Pantheon [104]. This reason leads to a similar advantage of the exponential $F(R)$ and some other models if we compare them with Λ CDM model [10].

The best fits of free model parameters in Table II differ between two models especially sharply (more than 3σ) for the matter density parameter Ω_m^0 . This difference for the Hubble constant H_0 is about 3σ , but the EGB estimation $H_0 = 65.90_{-1.54}^{+1.48}$ km/(sMpc) is essentially lower.

Hence, we may conclude that the EGB model (28) under the important constraints (7) on the speed of gravitational waves successfully fits well the latest cosmological data, including Pantheon+ SNe Ia, $H(z)$, CMB and DESI BAO data. This EGB model has an essential advantage when comparing with the Λ CDM model in $\min \chi^2$ and if we use Akaike and Bayesian information criteria.

Acknowledgments

This work was partially supported by the program Unidad de Excelencia Maria de Maeztu CEX2020-001058-M, Spain (S.D.O).

-
- [1] Planck collaboration: N. Aghanim *et al.*, *Astron. Astrophys.* **641** (2020), A6 [arXiv:1807.06209 [astro-ph.CO]].
- [2] D. Scolnic *et al.*, *Astrophys. J.* 938 (2022) 113, arXiv:2112.03863.
- [3] DESI collaboration, A. G. Adame *et al.* [DESI], [arXiv:2404.03002 [astro-ph.CO]]; R. Calderon *et al.*, *JCAP* **10** (2024) 048, arXiv:2405.04216; K. Lodha *et al.*, arXiv:2405.13588.
- [4] M. Abdul Karim *et al.* [DESI], [arXiv:2503.14738 [astro-ph.CO]].
- [5] A.G. Riess, W. Yuan, L.M. Macri and D. Scolnic, *Astrophys. J. Lett.* **908** (2021), L6, arXiv:2112.04510 [astro-ph.CO]. 131 (2021) 102605, arXiv:2008.11284.
- [6] S. Nojiri, S. D. Odintsov and V. K. Oikonomou, *Phys. Rept.* **692** (2017) 1 [arXiv:1705.11098 [gr-qc]].
- [7] S. Capozziello, M. De Laurentis, *Phys. Rept.* **509**, 167 (2011); V. Faraoni and S. Capozziello, *Fundam. Theor. Phys.* **170** (2010).
- [8] S. Nojiri, S.D. Odintsov, *eConf C0602061*, 06 (2006) [Int. J. Geom. Meth. Mod. Phys. **4**, 115 (2007)].
- [9] S. Nojiri, S.D. Odintsov, *Phys. Rept.* **505**, 59 (2011);
- [10] S. D. Odintsov, D. Saez-Chillon Gomez and G. S. Sharov, arXiv:2412.09409.
- [11] W. M. Dai, Y. Z. Ma and H. J. He, *Phys. Rev. D* **102** (2020), 121302 doi:10.1103/PhysRevD.102.121302 [arXiv:2003.03602 [astro-ph.CO]].
- [12] H. J. He, Y. Z. Ma and J. Zheng, *JCAP* **11** (2020), 003 doi:10.1088/1475-7516/2020/11/003 [arXiv:2003.12057 [hep-ph]].
- [13] Y. Nakai, M. Suzuki, F. Takahashi and M. Yamada, *Phys. Lett. B* **816** (2021), 136238 doi:10.1016/j.physletb.2021.136238 [arXiv:2009.09754 [astro-ph.CO]].
- [14] E. Di Valentino, A. Mukherjee and A. A. Sen, *Entropy* **23** (2021) no.4, 404 doi:10.3390/e23040404 [arXiv:2005.12587 [astro-ph.CO]].
- [15] P. Agrawal, G. Obied and C. Vafa, *Phys. Rev. D* **103** (2021) no.4, 043523 doi:10.1103/PhysRevD.103.043523 [arXiv:1906.08261 [astro-ph.CO]].
- [16] W. Yang, S. Pan, E. Di Valentino, R. C. Nunes, S. Vagnozzi and D. F. Mota, *JCAP* **09** (2018), 019 doi:10.1088/1475-7516/2018/09/019 [arXiv:1805.08252 [astro-ph.CO]].
- [17] G. Ye and Y. S. Piao, *Phys. Rev. D* **101** (2020) no.8, 083507 doi:10.1103/PhysRevD.101.083507 [arXiv:2001.02451 [astro-ph.CO]].
- [18] S. Vagnozzi, F. Pacucci and A. Loeb, [arXiv:2105.10421 [astro-ph.CO]].
- [19] H. Desmond, B. Jain and J. Sakstein, *Phys. Rev. D* **100** (2019) no.4, 043537 [erratum: *Phys. Rev. D* **101** (2020) no.6, 069904; erratum: *Phys. Rev. D* **101** (2020) no.12, 129901] doi:10.1103/PhysRevD.100.043537 [arXiv:1907.03778 [astro-ph.CO]].
- [20] E. Ó Colgáin, M. H. P. M. van Putten and H. Yavartanoo, *Phys. Lett. B* **793** (2019), 126-129 doi:10.1016/j.physletb.2019.04.032 [arXiv:1807.07451 [hep-th]].
- [21] S. Vagnozzi, *Phys. Rev. D* **102** (2020) no.2, 023518 doi:10.1103/PhysRevD.102.023518 [arXiv:1907.07569 [astro-ph.CO]].
- [22] C. Krishnan, E. Ó. Colgáin, Ruchika, A. A. Sen, M. M. Sheikh-Jabbari and T. Yang, *Phys. Rev. D* **102** (2020) no.10, 103525 doi:10.1103/PhysRevD.102.103525 [arXiv:2002.06044 [astro-ph.CO]].
- [23] E. Ó. Colgáin and H. Yavartanoo, *Phys. Lett. B* **797** (2019), 134907 doi:10.1016/j.physletb.2019.134907 [arXiv:1905.02555 [astro-ph.CO]].
- [24] S. Vagnozzi, *Phys. Rev. D* **104** (2021) no.6, 063524 doi:10.1103/PhysRevD.104.063524 [arXiv:2105.10425 [astro-ph.CO]].
- [25] B. H. Lee, W. Lee, E. Ó. Colgáin, M. M. Sheikh-Jabbari and S. Thakur, [arXiv:2202.03906 [astro-ph.CO]].
- [26] C. Krishnan, R. Mohayaee, E. Ó. Colgáin, M. M. Sheikh-Jabbari and L. Yin, *Class. Quant. Grav.* **38** (2021) no.18, 184001 doi:10.1088/1361-6382/ac1a81 [arXiv:2105.09790 [astro-ph.CO]].
- [27] G. Ye, J. Zhang and Y. S. Piao, [arXiv:2107.13391 [astro-ph.CO]].
- [28] G. Ye and Y. S. Piao, [arXiv:2202.10055 [astro-ph.CO]].
- [29] L. Verde, T. Treu and A. G. Riess, *Nature Astron.* **3**, 891 doi:10.1038/s41550-019-0902-0 [arXiv:1907.10625 [astro-ph.CO]].
- [30] N. Menci, S. A. Adil, U. Mukhopadhyay, A. A. Sen and S. Vagnozzi, *JCAP* **07** (2024), 072 doi:10.1088/1475-7516/2024/07/072 [arXiv:2401.12659 [astro-ph.CO]].
- [31] S. A. Adil, U. Mukhopadhyay, A. A. Sen and S. Vagnozzi, *JCAP* **10** (2023), 072 doi:10.1088/1475-7516/2023/10/072 [arXiv:2307.12763 [astro-ph.CO]].
- [32] A. Reeves, L. Herold, S. Vagnozzi, B. D. Sherwin and E. G. M. Ferreira, *Mon. Not. Roy. Astron. Soc.* **520** (2023) no.3, 3688-3695 doi:10.1093/mnras/stad317 [arXiv:2207.01501 [astro-ph.CO]].
- [33] F. Ferlito, S. Vagnozzi, D. F. Mota and M. Baldi, *Mon. Not. Roy. Astron. Soc.* **512** (2022) no.2, 1885-1905 doi:10.1093/mnras/stac649 [arXiv:2201.04528 [astro-ph.CO]].
- [34] S. Vagnozzi, L. Visinelli, P. Brax, A. C. Davis and J. Sakstein, *Phys. Rev. D* **104** (2021) no.6, 063023 doi:10.1103/PhysRevD.104.063023 [arXiv:2103.15834 [hep-ph]].

- [35] E. Di Valentino, S. Gariazzo, O. Mena and S. Vagnozzi, *JCAP* **07** (2020) no.07, 045 doi:10.1088/1475-7516/2020/07/045 [arXiv:2005.02062 [astro-ph.CO]].
- [36] E. Di Valentino, A. Melchiorri, O. Mena and S. Vagnozzi, *Phys. Dark Univ.* **30** (2020), 100666 doi:10.1016/j.dark.2020.100666 [arXiv:1908.04281 [astro-ph.CO]].
- [37] M. A. Sabogal, E. Silva, R. C. Nunes, S. Kumar, E. Di Valentino and W. Giarè, *Phys. Rev. D* **110** (2024) no.12, 123508 doi:10.1103/PhysRevD.110.123508 [arXiv:2408.12403 [astro-ph.CO]].
- [38] W. Giarè, M. A. Sabogal, R. C. Nunes and E. Di Valentino, *Phys. Rev. Lett.* **133** (2024) no.25, 251003 doi:10.1103/PhysRevLett.133.251003 [arXiv:2404.15232 [astro-ph.CO]].
- [39] S. Nojiri and S. D. Odintsov, *Phys. Rev. D* **68** (2003), 123512 doi:10.1103/PhysRevD.68.123512 [arXiv:hep-th/0307288 [hep-th]].
- [40] S. Capozziello, V. F. Cardone and A. Troisi, *Phys. Rev. D* **71** (2005), 043503 doi:10.1103/PhysRevD.71.043503 [arXiv:astro-ph/0501426 [astro-ph]].
- [41] J. c. Hwang and H. Noh, *Phys. Lett. B* **506** (2001), 13-19 doi:10.1016/S0370-2693(01)00404-X [arXiv:astro-ph/0102423 [astro-ph]].
- [42] Y. S. Song, W. Hu and I. Sawicki, *Phys. Rev. D* **75** (2007), 044004 doi:10.1103/PhysRevD.75.044004 [arXiv:astro-ph/0610532 [astro-ph]].
- [43] T. Faulkner, M. Tegmark, E. F. Bunn and Y. Mao, *Phys. Rev. D* **76** (2007), 063505 doi:10.1103/PhysRevD.76.063505 [arXiv:astro-ph/0612569 [astro-ph]].
- [44] G. J. Olmo, *Phys. Rev. D* **75** (2007), 023511 doi:10.1103/PhysRevD.75.023511 [arXiv:gr-qc/0612047 [gr-qc]].
- [45] I. Sawicki and W. Hu, *Phys. Rev. D* **75** (2007), 127502 doi:10.1103/PhysRevD.75.127502 [arXiv:astro-ph/0702278 [astro-ph]].
- [46] V. Faraoni, *Phys. Rev. D* **75** (2007), 067302 doi:10.1103/PhysRevD.75.067302 [arXiv:gr-qc/0703044 [gr-qc]].
- [47] S. Carloni, P. K. S. Dunsby and A. Troisi, *Phys. Rev. D* **77** (2008), 024024 doi:10.1103/PhysRevD.77.024024 [arXiv:0707.0106 [gr-qc]].
- [48] S. Nojiri and S. D. Odintsov, *Phys. Lett. B* **657** (2007), 238-245 doi:10.1016/j.physletb.2007.10.027 [arXiv:0707.1941 [hep-th]].
- [49] N. Deruelle, M. Sasaki and Y. Sendouda, *Prog. Theor. Phys.* **119** (2008), 237-251 doi:10.1143/PTP.119.237 [arXiv:0711.1150 [gr-qc]].
- [50] S. A. Appleby and R. A. Battye, *JCAP* **05** (2008), 019 doi:10.1088/1475-7516/2008/05/019 [arXiv:0803.1081 [astro-ph]].
- [51] P. K. S. Dunsby, E. Elizalde, R. Goswami, S. Odintsov and D. S. Gomez, *Phys. Rev. D* **82** (2010), 023519 doi:10.1103/PhysRevD.82.023519 [arXiv:1005.2205 [gr-qc]].
- [52] S. Nojiri and S. D. Odintsov, *Phys. Lett. B* **631** (2005) 1, [hep-th/0508049].
- [53] A. de la Cruz-Dombriz and D. Saez-Gomez, *Class. Quant. Grav.* **29** (2012) 245014, [arXiv:1112.4481].
- [54] M. Benetti, S. Santos da Costa, S. Capozziello, J.S. Alcaniz and M. De Laurentis, *Int. J. Mod. Phys. D* **27** (2018) 1850084, arXiv:1803.00895
- [55] S. Lee and G. Tumurtushaa, *JCAP* **06** (2020) 029, [arXiv:2001.07021].
- [56] G. Navó and E. Elizalde, *Int. J. Geom. Meth. Mod. Phys.* **17** (2020) no.11, 2050162, [arXiv:2007.11507].
- [57] S.D. Odintsov, V.K. Oikonomou, F.P. Fronimos and K.V. Fasoulakos, *Phys. Rev. D* **102** (2020) 104042, [arXiv:2010.13580]
- [58] M. De Laurentis, M. Paoletta and S. Capozziello, *Phys. Rev. D* **91** (2015) no.8, 083531 doi:10.1103/PhysRevD.91.083531 [arXiv:1503.04659 [gr-qc]].
- [59] V.K. Oikonomou, *Int. J. Mod. Phys. D* **27** (2018) 1850059, [arXiv:1711.03389].
- [60] E. Elizalde, A. N. Makarenko, V. V. Obukhov, K. E. Osetrin, and A. E. Filippov, *Phys. Lett. B* **644** (2007) 1, [hep-th/0611213].
- [61] S. A. Pavluchenko and A. V. Toporensky, *Mod. Phys. Lett. A* **24** (2009), 513, [arXiv:0811.0558].
- [62] D. Chirkov, A. Giacomini, S. A. Pavluchenko, A. Toporensky. *Eur. Phys. J. C* **81**, (2021), 136, [arXiv:2012.03517].
- [63] S. Kawai, M.-a. Sakagami and J. Soda, *Phys. Lett. B* **437**, 284 (1998), [gr-qc/9802033].
- [64] S. Alexeyev, A. Toporensky and V. Ustiansky, *Class. Quant. Grav.* **17** (2000) 2243. [arXiv:gr-qc/9912071].
- [65] S. Nojiri, S. D. Odintsov and M. Sasaki, *Phys. Rev. D* **71** (2005) 123509, [hep-th/0504052].
- [66] S. Nojiri, S. D. Odintsov and M. Sami, *Phys. Rev. D* **74** (2006) 046004, [hep-th/0605039].
- [67] G. Cognola, E. Elizalde, S. Nojiri, S. Odintsov and S. Zerbini, *Phys. Rev. D* **75** (2007) 086002, [hep-th/0611198].
- [68] K. Bamba, A. N. Makarenko, A. N. Myagky and S. D. Odintsov, *JCAP* **1504** (2015) 001, [arXiv:1411.3852 [hep-th]].
- [69] Z. K. Guo and D. J. Schwarz, *Phys. Rev. D* **80** (2009) 063523, [arXiv:0907.0427 [hep-th]].
- [70] Z. K. Guo and D. J. Schwarz, *Phys. Rev. D* **81** (2010) 123520, [arXiv:1001.1897 [hep-th]].
- [71] P. X. Jiang, J. W. Hu and Z. K. Guo, *Phys. Rev. D* **88** (2013) 123508, [arXiv:1310.5579 [hep-th]].
- [72] S. Koh, B.H. Lee, W. Lee, and G. Tumurtushaa, *Phys. Rev. D* **90** (2014) 063527, [arXiv:1404.6096].
- [73] Z. Yi, Y. Gong and M. Sabir, *Phys. Rev. D* **98** (2018) no.8, 083521, [arXiv:1804.09116 [gr-qc]].
- [74] S. D. Odintsov and V. K. Oikonomou, *Phys. Rev. D* **98** (2018) no.4, 044039, [arXiv:1808.05045 [gr-qc]].
- [75] S. Nojiri, S. Odintsov, V. Oikonomou, N. Chatzarakis and T. Paul, *Eur. Phys. J. C* **79** (2019), no.7, 565, [arXiv:1907.00403].
- [76] S. D. Odintsov and V. K. Oikonomou, *Phys. Lett. B* **797** (2019) 134874, [arXiv:1908.07555 [gr-qc]].
- [77] S. D. Odintsov, V. K. Oikonomou and F. P. Fronimos, *Nucl. Phys. B* **958** (2020), 115135, [arXiv:2003.13724 [gr-qc]].
- [78] S. D. Odintsov and V. K. Oikonomou, *Phys. Lett. B* **805** (2020), 135437 [arXiv:2004.00479 [gr-qc]].
- [79] S. D. Odintsov, V. K. Oikonomou and F. P. Fronimos, *Annals Phys.* **420** (2020), 168250, [arXiv:2007.02309 [gr-qc]].
- [80] V. K. Oikonomou and F. P. Fronimos, *EPL* **131** (2020) 3, 30001, [arXiv:2007.11915 [gr-qc]].

- [81] S. D. Odintsov, V. K. Oikonomou, F. P. Fronimos and S. A. Venikoudis, *Phys. Dark Univ.* **30** (2020), 100718, [arXiv:2009.06113 [gr-qc]].
- [82] S. Nojiri, S. D. Odintsov and V. K. Oikonomou, *Phys. Rev. D* **109** (2024) no.4, 044046, [arXiv:2311.06932 [gr-qc]].
- [83] V. K. Oikonomou, P. Tsyba and O. Razina, *Annals Phys.* **462** (2024), 169597 [arXiv:2401.11273].
- [84] V. K. Oikonomou, *Phys. Lett. B* **856** (2024), 138890, [arXiv:2407.12155].
- [85] I. Fomin, *Eur. Phys. J. C* **80** (2020) 1145, [arXiv:2004.08065 [gr-qc]].
- [86] E. O. Pozdeeva, *Eur. Phys. J. C* **80** (2020) 612, [arXiv:2005.10133 [gr-qc]].
- [87] E. O. Pozdeeva, M. R. Gangopadhyay, M. Sami, A. V. Toporensky, S. Yu. Vernov *Phys. Rev. D* **102** (2020), 043525, arXiv:2006.08027.
- [88] E. O. Pozdeeva, M. A. Skugoreva, A. V. Toporensky and S. Y. Vernov, *JCAP* **09** (2024), 050, [arXiv:2403.06147].
- [89] V. K. Oikonomou and F. P. Fronimos, *Eur. Phys. J. Plus* **135** (2020) no.11, 917, [arXiv:2011.03828 [gr-qc]].
- [90] E. O. Pozdeeva, M. Sami, A. V. Toporensky and S. Y. Vernov, *Phys. Rev. D* **100** (2019) no.8, 083527, [arXiv:1905.05085].
- [91] S. Vernov and E. Pozdeeva. *Universe* **2021**, 7(5), 149, [arXiv:2104.11111].
- [92] S.D. Odintsov, V.K. Oikonomou and F.P. Fronimos, *Class. Quant. Grav.* **38** (2021), 7, 075009, [arXiv:2102.02239].
- [93] S. D. Odintsov, D. S. C. Gómez and G. S. Sharov, *Phys. Dark Univ.* **37** (2022) 101100, [arXiv:2207.08513].
- [94] S. Nojiri, S. D. Odintsov, T. Paul, *Phys. Dark Univ.* **35** (2022) 100984, [arXiv:2202.02695].
- [95] A. Codello and R. K. Jain, *Class. Quant. Grav.* **33** (2016) no.22, 225006 doi:10.1088/0264-9381/33/22/225006 [arXiv:1507.06308 [gr-qc]].
- [96] J. T. Wheeler, *Nucl. Phys. B.* **268** (1986), 737.
- [97] B. P. Abbott *et al.* [LIGO Scientific and Virgo], *Phys. Rev. Lett.* **119** (2017) no.16, 161101 doi:10.1103/PhysRevLett.119.161101 [arXiv:1710.05832 [gr-qc]].
- [98] Planck collaboration: P. A. R. Ade *et al.* *Astron. Astrophys.* **571** (2014), A16, [arXiv:1303.5076].
- [99] S. D. Odintsov, D. Saez-Chillon Gomez and G. S. Sharov, *Phys. Rev. D* **101** (2020) no.4, 044010, [arXiv:2001.07945].
- [100] S. D. Odintsov, D. Sáez-Chillón Gómez and G. S. Sharov, *Eur. Phys. J. C* **77** (2017) no.12, 862, [arXiv:1709.06800].
- [101] S. D. Odintsov, D. Sáez-Chillón Gómez and G. S. Sharov, *Phys. Dark Univ.* **46** (2024) 101558, [arXiv:2406.08831 [gr-qc]].
- [102] L. Chen, Q.-G. Huang and K. Wang, *J. Cosmol. Astropart. Phys.* **1902** (2019) 028, arXiv:1808.05724.
- [103] A. R. Liddle, *Mon. Not. Roy. Astron. Soc.* **377** (2007), L74-L78, [arXiv:astro-ph/0701113 [astro-ph]].
- [104] D. M. Scolnic *et al.*, *Astrophys. J.* **859** (2018) 101, arXiv:1710.00845.